DISCRETE AND CONTINUOUS
DYNAMICAL SYSTEMS SERIES B
Volume **20**, Number **7**, September **2015**

doi:10.3934/dcdsb.2015.20.1983

pp. **1983–2000**

REORIENTATION OF SMECTIC A LIQUID CRYSTALS BY MAGNETIC FIELDS

Carlos J. García-Cervera

Mathematics Department
University of California
Santa Barbara, CA 93106, USA

Sookyung Joo

Department of Mathematics and Statistics
Old Dominion University
Norfolk, VA 23529, USA

(Communicated by Qi Wang)

Abstract. We consider the de Gennes' smectic A free energy with a complex order parameter in order to study the influence of magnetic fields on the smectic layers in the strong field limit as well as near the critical field. In previous work by the authors [6], the critical field and a description of the layer undulations at the instability were obtained using Γ-convergence and bifurcation theory. It was proved that the critical field is lowered by a factor of $\sqrt{\pi}$ compared to the classical Helfrich Hurault theory by using natural boundary conditions for the complex order parameter, but still with strong anchoring condition for the director. In this paper, we present numerical simulations for undulations at the critical field as well as the layer and director configurations well above the critical field. We show that the estimate of the critical field and layer configuration at the critical field agree with the analysis in [6]. Furthermore, the changes in smectic order density as well as layer and director will be illustrated numerically as the field increases well above the critical field. This provides the smectic layers' melting along the bounding plates where the layers are fixed. In the natural case, at a high field, we prove that the directors align with the applied field and the layers are homeotropically aligned in the domain, keeping the smectic order density at a constant in L^2.

1. **Introduction.** In a previous article [6], the authors have investigated the undulation phenomena induced by magnetic fields in smectic A liquid crystals using the complex de Gennes model. Using bifurcation theory and Γ-convergence, the authors found the critical magnetic field and were able to describe the director and the smectic layers at the onset of undulations. The model used in [6] for the numerical study assumes that the density of the smectic layers is constant. In this paper, we consider the full model, in which the density is allowed to fluctuate, and show that the critical field and other qualitative features are consistent with the analytical results given in [6]. This models can describe the director, layer phase and density

2010 *Mathematics Subject Classification.* Primary: 82D30, 35Q56; Secondary: 65Z05.

Key words and phrases. Smectic liquid crystal, critical magnetic field, layer undulations, de Gennes model, high field regime.

C.J. García-Cervera is supported by NSF grants DMS-0645766 and DMS-0908538.

S. Joo is supported by NSF grant DMS-1120637.

profiles well above the critical field as well as at the onset of undulations. We study the phenomenon numerically, and obtain an analytic expression for the minimizer in the high field regime.

We consider a smectic A liquid crystal confined between two flat plates and uniformly aligned in a way that the smectic layers are parallel to the bounding plates and the directors are aligned homeotropically, that is, perpendicular to the smectic layers. If a magnetic field is applied in the direction parallel to the smectic layers, an instability occurs above a threshold magnetic field. When the magnetic field reaches this critical threshold, periodic layer undulations are observed. This phenomenon is called the Helfrich-Hurault effect (see [10] and [11]).

We consider a two dimensional rectangular domain and impose periodic boundary conditions on the lateral boundaries. For the liquid crystal director, strong anchoring conditions are employed on the top and bottom bounding plates. We consider two types of boundary conditions for the smectic order parameter: Dirichlet and Neumann (or natural) boundary conditions. Employing Dirichlet boundary conditions fixes the layers flat at the bounding plates. In this case, we showed that the critical field is the same as in the classical Helfrich-Hurault theory. Furthermore, as in the classic Helfrich-Hurault theory, the maximum undulation amplitude occurs in the middle of the cell and decreases near the bounding plates at the onset of undulations; the perturbation increases as the field increases. However, when using natural boundary conditions for the smectic order parameter, the boundary layers are allowed to fluctuate, which lowers the critical field and increases the undulation amplitude at the onset of the undulations.

With the analysis presented in [6], the authors were able to connect the model (4) below with two simplified models used for the study of undulations in lateral systems: 1) The classical Helfrich-Hurault model, and 2) the model introduced by Lavrentovich and collaborators [12, 19].

In the classical Helfrich-Hurault theory, one identifies the director and layer normal. Writing the displacement of the layers as $u = y - \nabla\phi$, where ϕ parametrizes the layer surface, the classical model is given by

$$\int_\Omega \left(\frac{K}{2} u_{xx}^2 + \frac{B}{2} u_z^2 - \frac{\chi_a H^2}{2} u_x^2 \right) dxdy. \tag{1}$$

This can be obtained as the Γ-limit of the functional (4) when Dirichlet boundary conditions are imposed, as established in [6]. Thus, it is not surprising that the estimate of the critical field and undulation profiles in [6] are identical to the results from the Helfrich-Hurault theory. In this case the critical field is given by

$$H_c^D \sim \left(\frac{K\pi}{\chi_a d_0 \lambda} \sqrt{\frac{r}{g}} \right)^{\frac{1}{2}}, \tag{2}$$

where the elastic length $\lambda = \sqrt{\frac{K}{Cq^2}}$ is of the order of the layer thickness. This value is the same as the one from the classical Helfrich-Hurault theory except for the appearance of $\sqrt{r/g}$. However, well above the critical field, our numerical simulations show differences between the director and the layer normal. Moreover, on some regions of the domain, the layer density gets close to zero at high fields. In particular, along the bounding plates, melting of the smectic layers occurs at high fields when Dirichlet boundary conditions are imposed, with leads to the development of nematic defects.

When natural boundary condition is employed, it was proved in [6] that the Γ-limit recovers the functional used in [12, 19], where a soft anchoring conditions is introduced as a penalty in the energy, again identifying the director and the layer normal. They showed using this model that a lower threshold in the magnetic field produces larger undulations, and these as less dependent on the vertical axis than those from the classical Helfrich-Hurault theory, as observed in their experiments. Our results on critical fields and undulation profiles can also explain the experiments in [12, 19]. The critical field in this case is given by

$$H_c^N \sim \left(\frac{K}{\chi_a d_0 \lambda}\sqrt{\frac{r}{g}}\right)^{\frac{1}{2}}. \tag{3}$$

One can see that imposing natural boundary conditions on the smectic order parameter reduces the critical field by a factor of $\sqrt{\pi}$. Note that in both Dirichlet and Neumann cases, a strong anchoring condition is imposed on the director.

From a physical point of view, determining the critical field is useful because among other things it allows one to estimate the value of the elastic length λ. In [12] and [14], the authors discussed this issue, and they found a discrepancy between the value of the elastic constants obtained from λ using the Helfrich-Hurault theory and the value obtained from the Lubensky-de Gennes theory [1]. Instead of $\lambda = (8.5 \pm 1.7)\mu m$, which is the value obtained in the classical theory, they measured λ independently and found that $\lambda = (2.9 \pm 0.1)\mu m$. From the discrepancies between H_c^D and H_c^N, one can see that the classical value of λ needs to be reduced by a factor of π. This can explain the correct value of λ obtained in [12].

We have proved also in [6] that under natural boundary conditions the vertical dependence of the undulation amplitudes is almost lost at the onset of the undulations as $\varepsilon \to 0$ where the small parameter ε is the ratio of the layer thickness to the sample thickness. Numerical simulations show a mismatch between the director and the layer normal near the boundary even at the onset of the undulations. This is not the case with the Dirichlet boundary condition on the smectic order parameter.

In [16], the authors proved that under very strong magnetic fields, a smectic A liquid crystal (with natural boundary conditions on the smectic order parameter) may not be in the nematic state. In fact, the strong magnetic field reorients the director to be parallel to the magnetic field inside the domain and the smectic layer density is kept away from zero. The results in [16] were our main motivation to study the director and smectic order parameter at high fields.

In section 2, the de Gennes free energy is introduced and a dimensionless small parameter ε is identified in the process of nondimensionalization. Estimates of the critical fields for both cases of Dirichlet and natural boundary conditions are presented. In section 3 we formulate the gradient flow of the de Gennes free energy and illustrate numerically the effect of magnetic fields on smectic liquid crystals. The director configuration, layer structure, and smectic order density profiles are shown for various magnetic field strengths. In the natural boundary condition case, we obtain analytically the director and layer structure of smectic A liquid crystals under very strong magnetic fields by studying the minimizers of de Gennes free energy in section 4. We prove that at high fields, the director is aligned parallel to the magnetic field and initially flat layers change to a vertically aligned uniform structure in order to accommodate the director configurations.

2. **Model and preliminary results.** We study the Landau-de Gennes energy [2] to understand the effect of an applied magnetic field on smectic A liquid crystals. The model, introduced by de Gennes, is described in terms of the director $\mathbf{n}$ and the complex order parameter $\psi = \rho(\mathbf{x})e^{iq\omega(\mathbf{x})}$ for the layered structure. The unit vector field $\mathbf{n}$, director field, represents the average direction of molecular alignment. The molecular mass density is defined by

$$\delta(\mathbf{x}) = \rho_0(\mathbf{x}) + \frac{1}{2}(\psi(\mathbf{x}) + \psi^*(\mathbf{x})) = \rho_0(\mathbf{x}) + \rho(\mathbf{x})\cos q\omega(\mathbf{x}),$$

where ρ_0 is a locally uniform mass density, $\rho(\mathbf{x})$ is the mass density of the smectic layers, and ω parametrizes the layers so that $\nabla\omega$ is the direction of the layer normal. Also, q is the wave number and $2\pi/q$ is the layer thickness. If $\psi \equiv 0$, then it corresponds to a state with no layered structure, so it is in a nematic phase. If $|\psi| = \rho$ is a nonzero constant, it corresponds to a smectic state throughout the domain.

In the one constant approximation case for the Oseen-Frank nematic energy, the total free energy is given by,

$$\mathcal{G}(\psi, \mathbf{n}) = \int_{\Omega_0} \left(C|\nabla\psi - iq\mathbf{n}\psi|^2 + K|\nabla\mathbf{n}|^2 + \frac{g}{2}\Big(|\psi|^2 - \frac{r}{g}\Big)^2 - \chi_a H^2(\mathbf{n}\cdot\mathbf{h})^2 \right) d\mathbf{x}. \tag{4}$$

The material parameters C, K, g, and temperature r are fixed positive constants and $\Omega_0 = (-L_0, L_0) \times (-d_0, d_0)$ is a rectangular domain. If ρ is a constant, then the first term of (4) becomes

$$\frac{Cq^2\rho^2}{2}|\nabla\omega - \mathbf{n}|^2.$$

This energy density vanishes when $\nabla\omega = \mathbf{n}$, which describes the configuration of smectic A liquid crystals. The last term in (4) is a contribution to the magnetic free energy density, where χ_a is the magnetic anisotropy, H is the magnitude of the magnetic field and $\mathbf{h}$ is a unit vector representing the direction of the applied field. We assume that $\chi_a > 0$. As a consequence, the director has a preferred orientation parallel to the direction of the applied magnetic field. The magnetic field is applied in the direction parallel to the layers. We shall assume that

$$\mathbf{h} = \mathbf{e}_1.$$

We define the dimensionless order parameter, $\varphi = \sqrt{\frac{q}{r}}\psi$, and do the change of variables $\bar{\mathbf{x}} = q\mathbf{x}$; then we obtain a nondimensionalized energy

$$\mathcal{G}(\varphi, \mathbf{n}) = \frac{Cr}{g}\int_\Omega \left(|\nabla\varphi - i\mathbf{n}\varphi|^2 + \widetilde{K}|\nabla\mathbf{n}|^2 + \frac{\widetilde{g}}{2}(1 - |\varphi|^2)^2 - \sigma(\mathbf{n}\cdot\mathbf{h})^2 \right) d\bar{\mathbf{x}}, \tag{5}$$

where

$$\widetilde{K} = \frac{Kg}{Cr}, \qquad \widetilde{g} = \frac{r}{Cq^2}, \qquad \sigma = \frac{\chi_a H^2 g}{Crq^2}, \tag{6}$$

and

$$\Omega = (-L, L) \times (-d, d), \quad L = qL_0, \quad d = qd_0.$$

Assuming $\mathbf{n} = (\sin\theta, \cos\theta)$, the uniformly layered state, $(\varphi_0, \theta_0) \equiv (\tilde{c}e^{iy}, 0)$, is a trivial critical point of $\mathcal{G}$ where $\tilde{c} \in \mathbb{C}$ such that $|\tilde{c}| = 1$. The second variation of $\mathcal{G}$

at the undeformed state, $\varphi_0 = \tilde{c}e^{iy}$, $\theta_0 = 0$, is

$$\frac{1}{2}\frac{g}{Cr}\frac{d^2}{dt^2}\mathcal{G}(\varphi_0 + t\varphi, t\theta)\Big|_{t=0} = \int_\Omega (|\varphi_x - i\theta\varphi_0|^2 + |\varphi_y - i\varphi|^2 + \widetilde{K}|\nabla\theta|^2 + 2\widetilde{g}[Re(\varphi_0\bar{\varphi})]^2 - \sigma|\theta|^2)\, d\bar{x}d\bar{y}. \tag{7}$$

The undeformed state, (θ_0, φ_0), is stable if the second variation is nonnegative. As in [16] and [6], we write

$$\varphi = i\varphi_0\phi. \tag{8}$$

Then the second variation above becomes

$$\int_\Omega (|\phi_x - \theta|^2 + |\phi_y|^2 + \widetilde{K}|\nabla\theta|^2 + 2\widetilde{g}[Im(\phi)]^2)\, d\bar{x}d\bar{y} - \sigma\int_\Omega |\theta|^2\, d\bar{x}d\bar{y}. \tag{9}$$

In order to find the critical value of σ, we minimize (9) over functions satisfying $\|\theta\|_2 = 1$. Note that in this case only the first four terms need to be considered in the minimization. Additionally, given a minimizer $\phi = \Re\{\phi\} + i\Im\{\phi\}$, the function $\widetilde{\phi} = \Re\{\phi\}$ is admissible, and has lower energy. Therefore one may assume that ϕ is a real-valued function. Thus we set

$$\mathcal{L}(\phi, \theta) = \int_{\bar{\Omega}} (|\phi_x - \theta|^2 + |\phi_y|^2 + \widetilde{K}|\nabla\theta|^2)\, d\bar{x}d\bar{y} \tag{10}$$

and consider two admissible sets, $\mathcal{A}^N$, and $\mathcal{A}^D$, defined by

$$\mathcal{A}^N = \{(\phi, \theta) \in H^1(U) \times H^1(U) : \|\theta\|_2 = 1, \theta(x, \pm d) = 0 \text{ for all } x\},$$

and

$$\mathcal{A}^D = \{(\phi, \theta) \in \mathcal{A}^N : \phi(x, \pm d) = 0 \text{ for all } x\},$$

respectively, where $U = \mathbb{R}/(-L + 2L\mathbb{Z}) \times (-d, d)$. A detailed analysis of the functional (9) in these two admissible sets was presented in the previous paper [6]. Note that $\mathcal{A}^D$ corresponds to the setting where the layers are fixed at the cell boundaries since ϕ is the layer and smectic mass density perturbation from the undeformed smectic state. On the other hand, we do not impose any constraint on the boundary values of the order parameter ϕ in $\mathcal{A}^N$, which leads to natural boundary conditions for the minimizer. The critical field σ_c^i for $i = D$ or $i = N$ is then defined by

$$\sigma_c^i = \inf_{(\phi,\theta)\in\mathcal{A}^i} \mathcal{L}(\phi, \theta). \tag{11}$$

We introduce now the following change of variables, which will help us obtain a dimensionless small parameter ε. This is the nondimensionalized energy used in [6] for the use of Γ-convergence. Setting

$$\widetilde{x} = \frac{1}{qd_0}\bar{x}, \qquad \widetilde{y} = \frac{1}{qd_0}\bar{y}, \qquad \phi(x, y) = qd_0\,\phi(\widetilde{x}, \widetilde{y}), \tag{12}$$

we write (10) as

$$\frac{\widetilde{K}}{\varepsilon}\int_{\widetilde{\Omega}} \left(\frac{1}{\varepsilon}(\phi_x - \theta)^2 + \frac{1}{\varepsilon}\phi_y^2 + \varepsilon|\nabla\theta|^2 - \tau\theta^2\right) d\widetilde{x}d\widetilde{y} =: \frac{\widetilde{K}}{\varepsilon}\mathcal{J}(\theta, \phi), \tag{13}$$

where

$$\varepsilon = \frac{\sqrt{\widetilde{K}}}{qd_0} = \frac{\lambda}{d_0}\sqrt{\frac{g}{r}} \ll 1 \qquad \text{and} \qquad \tau = \frac{\sigma}{\varepsilon}. \tag{14}$$

Here the dimensionless domain is

$$\widetilde{\Omega} = (-r, r) \times (-1, 1) \quad \text{where} \quad r = \frac{L}{d}. \tag{15}$$

Since λ is of the order of the smectic layer thickness and thus ε in (14) is the ratio of the layer thickness to the cell thickness, we may assume that $\varepsilon \ll 1$. In fact, the values $d_0 = 1mm$ and $\lambda = 20\mathring{A}$ are employed in [3].

Functional (13) was extensively studied in [6] to obtain sharp estimates of the critical field and the undulation modes under both Dirichlet and Natural boundary conditions imposed on ϕ. When Dirichlet boundary conditions are used, the analysis recovers results that are consistent with the classical Helfrich-Hurault theory. However, with natural boundary condition, we have found that the critical field is lowered by a factor of $1/\pi$; the undulation profiles have a weak dependence on the vertical coordinate and have larger amplitudes, as expected from the experiments in [19].

The sharp estimates of the critical fields defined in (11) for Dirichlet and Natural boundary conditions on the complex order parameter obtained in [6] are given by

$$\sigma_c^D \approx \pi\varepsilon \qquad \text{and} \qquad \sigma_c^N \approx \varepsilon \tag{16}$$

for ε small, which is given in (14). In terms of the original elastic constants, the critical fields are estimated in (2) and (3) from (6).

3. **Numerical simulations.** We consider the gradient flow (in L^2) of the energy (5) and study the behavior of the solutions with both Dirichlet and natural boundary conditions. The gradient flow equations are

$$\begin{aligned} \frac{\partial \mathbf{n}}{\partial t} &= \Pi_{\mathbf{n}} \left(\widetilde{K}\Delta \mathbf{n} - \Im[\varphi(\nabla\varphi)^*] - |\varphi|^2\mathbf{n} + \sigma(\mathbf{n}\cdot\mathbf{h})\mathbf{h} \right), \\ \frac{\partial \varphi}{\partial t} &= \Delta\varphi - 2i\mathbf{n}\cdot\nabla\varphi - i(\nabla\cdot\mathbf{n})\varphi - \varphi + \widetilde{g}(1-|\varphi|^2)\varphi, \end{aligned} \tag{17}$$

where we have defined, for a given vector $f \in \mathbb{R}^3$, the orthogonal projection onto the plane orthogonal to the vector $\mathbf{n}$ as

$$\Pi_n(f) = f - (\mathbf{n}\cdot f)\mathbf{n}.$$

This projection appears as a result of the constraint $|\mathbf{n}| = 1$. Motivated from the numerical simulations for Landau-Lifshitz equation of micromagnetics in the high damping limit [4], and the heat-flow of harmonic maps [20], we write this equation as

$$\frac{\partial \mathbf{n}}{\partial t} = -\mathbf{n} \times \left(\mathbf{n} \times \left(\widetilde{K}\Delta \mathbf{n} - \Im[\varphi(\nabla\varphi)^*] - |\varphi|^2\mathbf{n} + \sigma(\mathbf{n}\cdot\mathbf{h})\mathbf{h} \right) \right) \tag{18}$$

and use the projection method introduced in [4]. We let f^* denote the complex conjugate of f.

As initial condition, we consider a small perturbation from the undeformed state. More precisely, for all $(x, y) \in \Omega$,

$$\begin{aligned} \mathbf{n}(x,y,0) &= \frac{(\epsilon u_1, 1+\epsilon u_2)}{|(\epsilon u_1, 1+\epsilon u_2)|}, \\ \varphi(x,y,0) &= e^{iy} + \epsilon\varphi_0, \end{aligned}$$

where a small number $\epsilon = 0.1$ and u_1, u_2, and φ_0 are arbitrarily chosen. We impose strong anchoring condition for the director field,

$$\mathbf{n}(x, \pm d, t) = \mathbf{e}_2 \tag{19}$$

and either a homogeneous Dirichlet boundary condition or a natural boundary condition on φ at the top and the bottom plates. The natural boundary condition on φ is

$$\frac{\partial \varphi}{\partial \nu}\Big|_{y=\pm d} = i\mathbf{n}\cdot\nu\varphi\Big|_{y=\pm d}.$$

Periodic boundary conditions are imposed for both $\mathbf{n}$ and φ in the x direction.

We use a Fourier spectral discretization in the x direction, and second order finite differences in the y direction. The fast Fourier transform is computed using the FFTW libraries [5]. For the temporal discretization, we combine a projection method for the variable $\mathbf{n}$ [4], with a semi-implicit scheme for φ: Given $(\varphi^k, \mathbf{n}^k)$, we solve

$$\frac{\mathbf{n}^* - \mathbf{n}^k}{\Delta t} = \widetilde{K}\Delta\mathbf{n}^* - \Im[\varphi^k(\nabla\varphi^k)^*] - |\varphi^k|^2\mathbf{n}^k + \sigma(\mathbf{n}^k\cdot\mathbf{h})\mathbf{h}, \tag{20}$$

$$\mathbf{n}^{k+1} = \frac{\mathbf{n}^*}{|\mathbf{n}^*|}, \tag{21}$$

$$\frac{\varphi^{k+1}-\varphi^k}{\Delta t} = \Delta\varphi^{k+1} - 2i\mathbf{n}^{k+1}\cdot\nabla\varphi^k - i(\nabla\cdot\mathbf{n}^{k+1})\varphi^k - \varphi^{k+1} + \widetilde{g}(1-|\varphi^k|^2)\varphi^k. \tag{22}$$

The second step (21) ensures that $|\mathbf{n}^{k+1}| = 1$ at each grid point. Note that $|\mathbf{n}^*| \neq 0$ in (21) since we consider the case where there are no point defects in the liquid crystal. The consistency and convergence of the projection method are given in [4]. The method is first order accurate in time and second order accurate in space due to the first order accuracy of the projection method (20)-(21). To solve the implicit system, we perform a discrete Fourier transform in the x direction. The resulting tridiagonal systems in the y direction are solved using Gauss elimination.

We take the domain size $L = 50$ and $d = 12.5$ as in [6]. The number of grid points in the x and y directions are 1024 and 512, respectively. Here we use parameters

$$K = 0.002, \quad C = 0.02, \quad g = 1, \quad r = 0.5, \quad \text{and} \quad q = 10,$$

and then we obtain from (6)

$$\widetilde{K} = 0.2, \quad \widetilde{g} = 0.25 \quad \text{and} \quad \varepsilon = \frac{\sqrt{\widetilde{K}}}{d} = 0.0358.$$

In Figure 1 we show the layer structures in response to various magnetic field strengths κ. In the figures we show the contour maps of φ since the level sets of φ represent the smectic layers. One can see that the undeformed state is stable for values of σ below the critical field σ_c. If σ increases and reaches σ_c, layer undulations occur.

We obtained the critical fields for both Dirichlet and Natural boundary conditions on the layer variable φ in [6]. With $d = 12.5$, the critical field σ_c^D under the Dirichlet boundary condition is approximately

$$\sigma_c^D \approx \varepsilon\pi = 0.1124.$$

Also, the critical field σ_c^N under the natural boundary condition is approximately

$$\sigma_c^N \approx \varepsilon = 0.0358.$$

The layer structures in the first and second rows of Fig. 1 confirm the prediction of the critical fields σ_c^D and σ_c^N for Dirichlet and natural boundary conditions on the

smectic order parameter φ. We also obtained the frequency of the undulations in [6]; In the Dirichlet case, the frequency is

$$\frac{\mu}{2\pi d} = \frac{1}{2\sqrt{2\pi d\sqrt{\widetilde{K}}}} \sim 0.085$$

where $2\pi/\mu = 2\pi/\mu_n$ is the frequency in the Fourier series, which was approximated by the formula $\varepsilon\mu^2 \sim \pi/2$ in [6]. Thus one may expect about $8 \sim 9$ frequencies in the domain size $2L = 100$ and this estimate is illustrated when $\sigma = 0.12$ in the left column of Fig. 1. In the general case, the frequency is independent of ε, and hence the frequency is the same as the one obtained in [6] where $\varepsilon = 1/12.5$ was used.

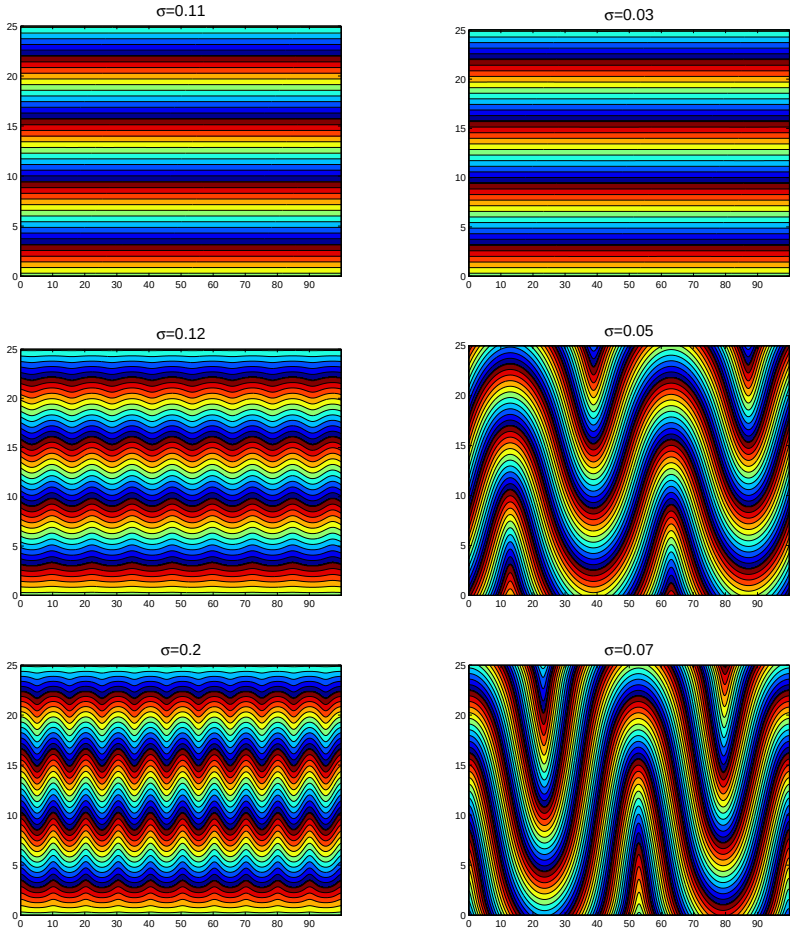

FIGURE 1. Contour plots of φ, the solution of the system (17), near the threshold. The first and the second column depict the layer when the Dirichlet and natural boundary conditions are imposed on φ, respectively.

At the onset of undulations, the smectic order density $|\varphi|$ may present differences between the Dirichlet and natural cases near the boundary of the domain. With

Dirichlet conditions on φ, the directors are perpendicular to the layers and the layers are rigid, $|\varphi| = 1$, everywhere in the domain (Fig. 2 (c)). In this case, the director is also kept at a homeotropic orientation (Fig. 2(e)) near the cell plates since the layers are fixed at the boundary. With natural boundary condition on φ however, the directors are realigned near the boundary (Fig. 2 (f)), having small perturbations from the homeotropic alignment, and thus lowering the energy, due to the presence of the magnetic field. This explains the lower critical field σ_c^N with the case of natural boundary condition. However, one may notice that the layers cannot accommodate the packing of the director at the top and bottom boundaries (Fig. 2 (b)), different from the Dirichlet case (Fig. 2 (a)). In [15], they expected some smectic layer melting in the vicinity of the bounding plates where they have frozen tilted layers. In fact, in order to compensate the frustration of the strong anchoring condition and tilted layer structures at the boundary, numerical simulations show smaller smectic order density, $|\varphi| < 1$ near the boundary as in Fig. 2 (d). The director is not identical with the layer normal near the vicinity of the bounding plates, which indicates that the model with two variables, the director and the smectic order parameter, is essential to recover the correct critical field σ_c^N.

The layer structure and its density and director profiles well above the critical field are illustrated in Fig. 3 and Fig. 4 when Dirichlet and natural boundary conditions on φ are considered, respectively. In the Dirichlet case, as the field increases, the sinusoidal layer undulations transforms to the saw-tooth profile shown in Fig. 3 (a), (d), (g). As σ increases, the magnetic energy becomes more prevalent. Hence, the director tends to be parallel to the magnetic field, which leads to an slight increase in the frequency of the undulations. Numerical simulations show that the frequencies of undulations increase with increasing σ, for moderate field strengths for both Dirichlet and natural boundary conditions. This can be observed, for example, for $\sigma = 0.12$ and $\sigma = 0.2$ in Fig. 1 for the Dirichlet case and for $\sigma = 0.1$ and $\sigma = 0.5$ in Fig. 4 for the natural case.

We note that, however, the period becomes larger with the strength of the magnetic field where we have used the Chen-Lubensky functional with constant density for the smectic A phase [7]. The presence of the second derivatives of the smectic order parameter in the Chen-Lubensky free energy makes change of the first order derivatives of the layer less preferable in the saw-tooth profiles of the undulations and thus is responsible for decreasing frequencies with any strengths of applied fields.

At higher fields, the frequencies start to decrease and layers become almost vertically aligned away from the cell plates. In order to accommodate the vertically aligned layer in the middle with the flat layer boundary condition, one can notice that the smectic layer melting appear along the boundary, as shown in Fig. 3 (e) and (f). The corresponding layer and director descriptions are given in Fig. 3 (b), (c), and (h), (i), respectively. Experiments in [12] also describe the sinusoidal shape at the onset of undulations and then at higher fields, the perturbation grows but appears to be independent of the vertical axis in the middle portion of the cell. At further higher field, the layers join the boundary discontinuously as in our Dirichlet case and form an array of dislocations [13].

With natural boundary conditions, the layers are tilted for all field strengths above the critical field (Fig. 1 and Fig. 4). This is achieved by making the smectic order density $|\varphi| < 1$ for some boundary regions where the director and layer normal differ. Nevertheless, $|\varphi|$ is away from 0. (See Fig. 4 (e) and (f).) Unlike the Dirichlet

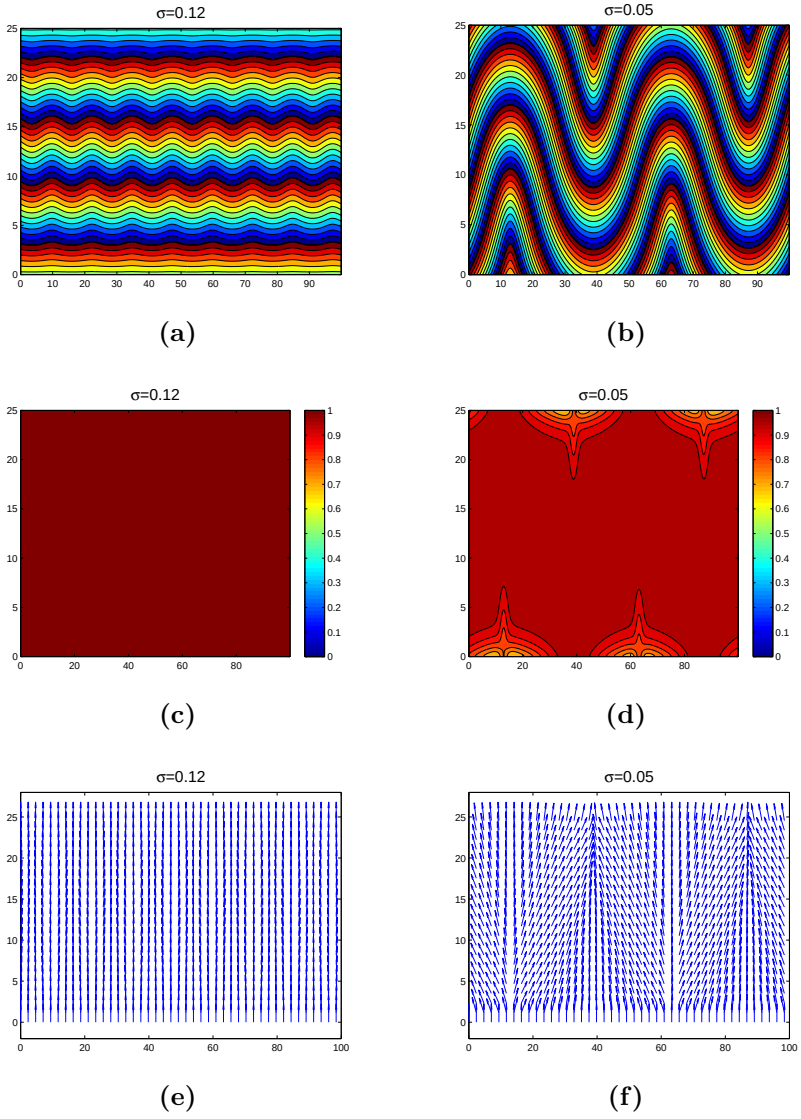

FIGURE 2. At the onset of undulations. Numerical simulations with strong anchoring conditions on the bounding plates. The first and the second columns are solutions to the system (17) with the Dirichlet and natural boundary conditions on φ, respectively. The first row depicts contour plots of the phase, the second row is the contour map of the dimensionless layer density $|\varphi|$, the third row shows the director profiles.

case, complete smectic melting does not occur with the natural boundary condition at any strengths of magnetic fields.

Furthermore, as σ increases well above the threshold, more areas of the domain have smectic density $|\varphi| \sim 1$, as in the case $\sigma = 2$ in Fig. 5. In the next section, we prove that as $\sigma \to \infty$, $|\varphi| \to 1$ and the layers tend to vertical lines. At extremely

high fields, the magnetic energy dominates and thus the directors are aligned parallel to the magnetic fields except at the jumps between $\mathbf{e}_1 = (1, 0)$ and $-\mathbf{e}_1$ and at the bounding plates. The number of jumps decreases with increasing magnetic fields in order to reduce the cost of the nematic energy (see (h) and (i) in Fig. 3 and Fig. 4). However, one should not expect the uniform state. Even though the magnetic field becomes extremely strong, there are still two jumps (Fig. 5) due to the periodic boundary conditions imposed on the director and φ. The analysis on sawtooth undulation profiles with two jump sets will appear in a future publication [8].

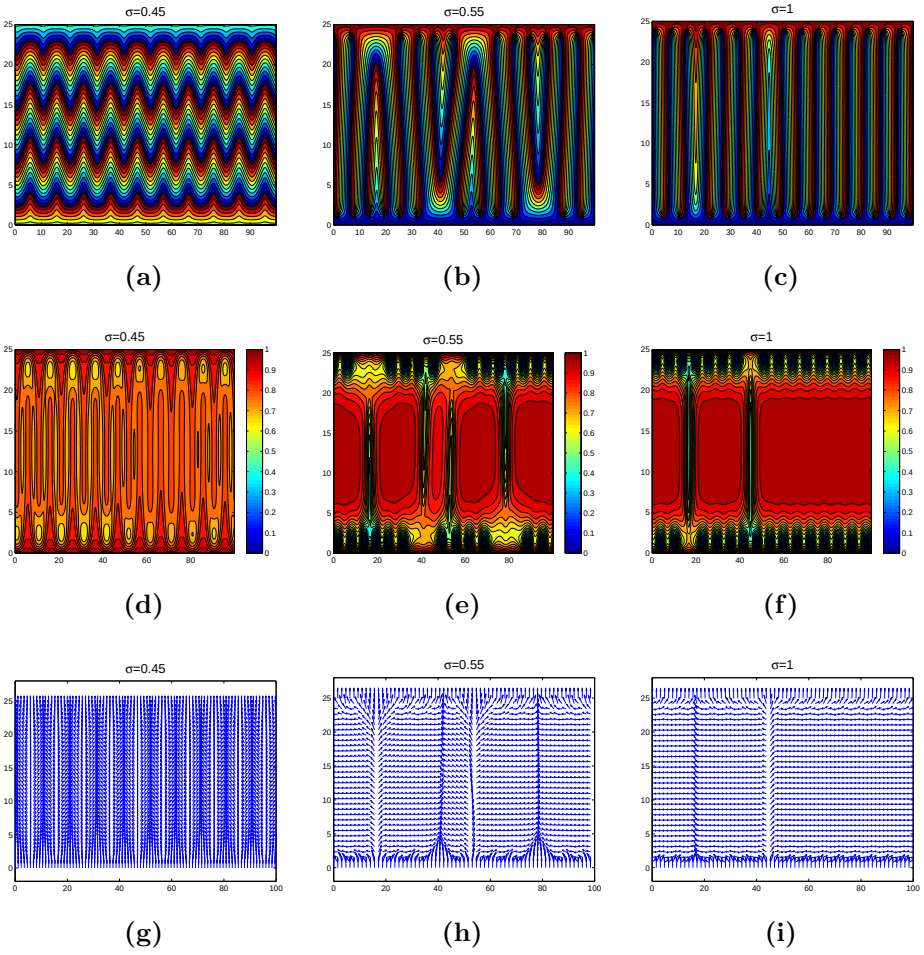

FIGURE 3. Numerical simulations with Dirichlet boundary conditions on φ on the bounding plates at various field strengths. The first row depicts contour plots of the phase, the second row is the contour map of the dimensionless layer density $|\varphi|$, the third row shows the director profiles.

4. **Configurations at high fields.** In this section, we only consider natural boundary conditions on φ at the top and bottom plates. The following theorem provides the behavior of the director for large field in $\mathbf{L}^2(\Omega)$. For this, we follow from the

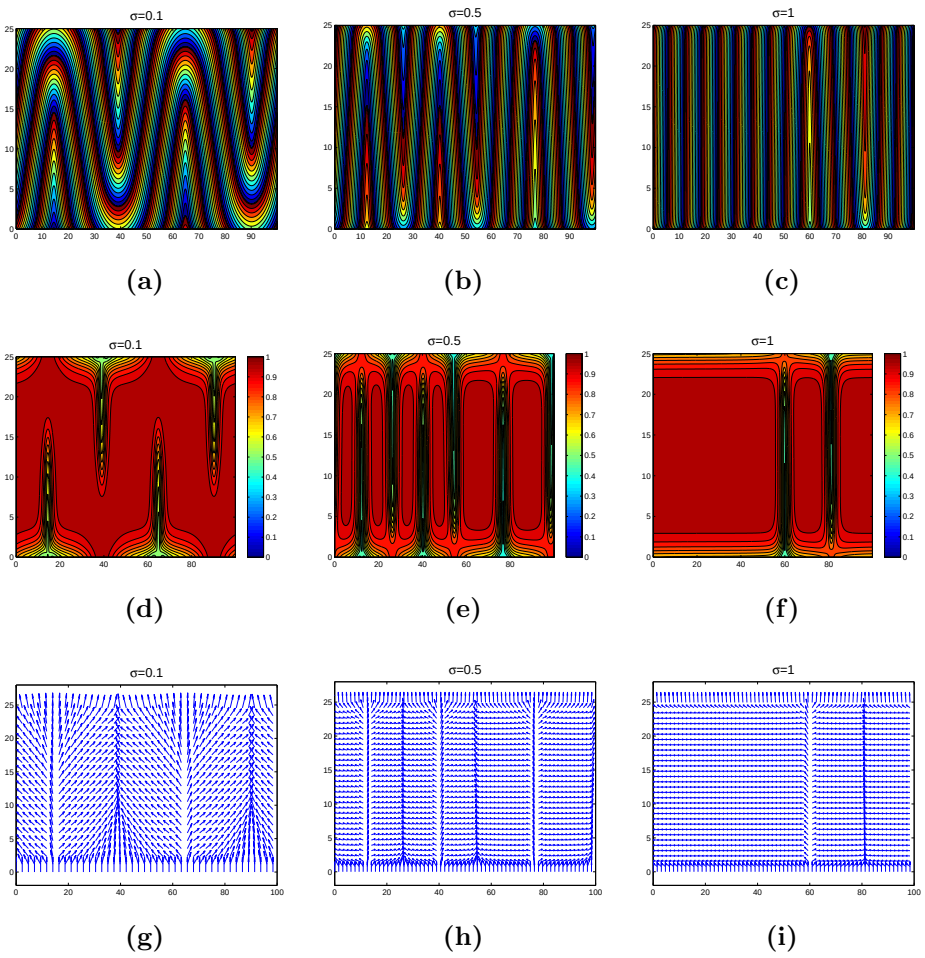

FIGURE 4. Numerical simulations with Neumann boundary conditions on φ on the bounding plates at various field strengths. The first row depicts contour plots of the phase, the second row is the contour map of the dimensionless layer density $|\varphi|$, the third row shows the director profiles.

statement and the proof of [16] closely. In [16], they proved that a liquid crystal will not be in the nematic phase no matter how strong the field is. We prove here that it is still in the smectic phase in most of the sample. The director will tend to align with the magnetic field under very strong fields except on the bounding plates where the directors are enforced by the strong anchoring conditions.

We write the energy (5) as

$$\mathcal{G}_\sigma(\varphi,\mathbf{n}) = \int_\Omega \left(|\nabla\varphi - i\mathbf{n}\varphi|^2 + \widetilde{K}|\nabla\mathbf{n}|^2 + \frac{\widetilde{g}}{2}(1-|\varphi|^2)^2 - \sigma(\mathbf{n}\cdot\mathbf{e}_1)^2 \right) dxdy. \quad (23)$$

We consider an admissible set

$$\begin{aligned} \mathcal{A} \quad = \quad & \{(\varphi,\mathbf{n}) \in W^{1,2}(\Omega)\times\mathbf{W}^{1,2}(\Omega,\mathcal{S}^1) : \mathbf{n}(x,\pm h) = \mathbf{e}_2 \text{ for all } x \\ & \mathbf{n}(-L,y) = \mathbf{n}(L,y) \text{ and } \varphi(-L,y) = \varphi(L,y)\}, \end{aligned} \quad (24)$$

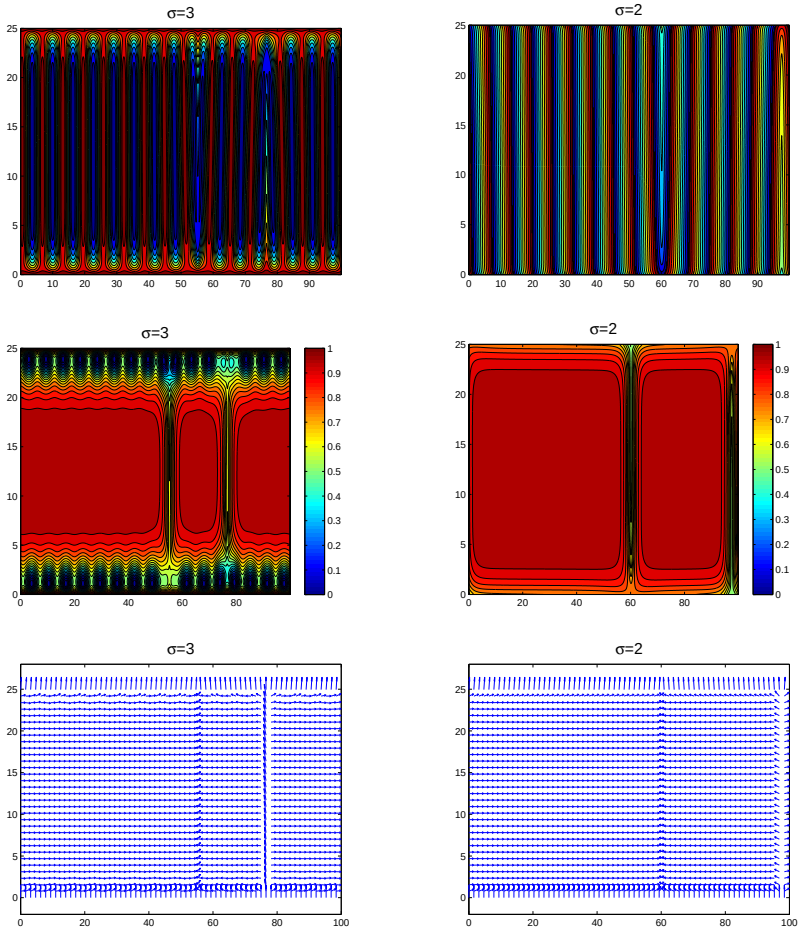

FIGURE 5. Well above the threshold. The first row depicts contour plots of the phase, the second row is the contour map of the dimensionless layer density $|\varphi|$, the third row shows the director profiles. The first and the second column depict the layer when Dirichlet and natural boundary conditions are imposed on φ, respectively.

where L is an integer multiple of π. We note that theorems in this section can be applied for the following admissible set, considered in [16],

$$\mathcal{B} = \{(\varphi, \mathbf{n}) \in W^{1,2}(\Omega) \times \mathbf{W}^{1,2}(\Omega, \mathcal{S}^1) : \mathbf{n} = \mathbf{e}_2 \text{ on } \partial\Omega\}.$$

Let $\mathbf{m}_\sigma$ be a global minimizer of the nematic liquid crystal energy,

$$\mathcal{F}_\sigma(\mathbf{n}) := \int_\Omega (\widetilde{K}|\nabla \mathbf{n}|^2 - \sigma n_1^2)\, dxdy. \tag{25}$$

In Lemma 5.5 of [16], they proved that a global minimizer $\mathbf{m}_\sigma$ does not change its sign for all field strengths, in particular, $\mathbf{m}_\sigma \to \mathbf{e}_1$ or $\mathbf{m}_\sigma \to -\mathbf{e}_1$ in $\mathbf{L}^2(\Omega)$ when strong anchoring conditions on $\mathbf{n}$ is imposed on $\partial\Omega$. We note that the same proof can be applied with periodic boundary conditions on the lateral side of the domain.

Thus we may assume that, passing to a subsequence,

$$\mathbf{m}_\sigma \to \mathbf{e}_1 \quad \text{in} \quad \mathbf{L}^2(\Omega) \quad \text{as} \quad \sigma \to \infty. \tag{26}$$

For smectic A, however, we note that a minimizer $\mathbf{n}_\sigma$ of the smectic A energy does change its sign as shown in Fig. 2(e) and (f). The director goes through the splay deformation at the undulation.

Before we state the main theorems in this section, we recall a few facts about functions of bounded variation. We let $BV(\Omega)$ denote the set of all $L^1(\Omega)$ functions u such that the total variation

$$\int_\Omega |Du| := \sup\left\{\int_\Omega u\,(div\zeta)\,dx : \zeta \in C_c^1(\Omega;\mathbb{R}^2), |\zeta| \le 1\right\} < \infty$$

and for $A \subset \mathbb{R}^2$,

$$BV(\Omega : A) = \{u \in BV(\Omega) : u(x) \in A \ \ a.e.\ x \in \Omega\}.$$

It is easy to see from the definition that if $\{u_n\} \subset L^1(\Omega)$ and $u_n \to u$ in $L^1(\Omega)$, then

$$\int_\Omega |Du| \le \liminf_{n\to\infty} \int_\Omega |Du_n|.$$

In addition, for any $R > 0$, the set

$$B_R := \left\{ u \in L^1(\Omega) \,\middle|\, \int_\Omega |u| + \int_\Omega |Du| \le R \right\}$$

is compact in $L^1(\Omega)$ [9].

The next theorem provides the behavior of the director configurations at high fields.

Theorem 4.1. *Let $(\varphi_\sigma, \mathbf{n}_\sigma)$ be a minimizer of $\mathcal{G}_\sigma(\varphi, \mathbf{n})$ in (23) for $(\varphi, \mathbf{n}) \in \mathcal{A}$ defined in (24).*

: *(a) For large σ, we have*

$$\mathcal{G}_\sigma(\varphi_\sigma, \mathbf{n}_\sigma) \le -|\Omega|\sigma + C\sqrt{\sigma},$$

for some positive constant $C = C(\widetilde{K}, \Omega)$.

: *(b) There exists $\mathbf{n}_\infty \in BV(\Omega : \{\pm\mathbf{e}_1\})$ such that (up to extraction of a subsequence) $\mathbf{n}_\sigma \to \mathbf{n}_\infty$ in $L^p(\Omega)$ for all $p < \infty$.*

Proof. For $\mathbf{n} \in \mathbf{W}^{1,2}(\Omega;\mathbb{S}^1)$, we may write

$$\mathcal{G}_\sigma(\varphi, \mathbf{n}) = \widetilde{\mathcal{G}}_\sigma(\varphi, \mathbf{n}) - \sigma|\Omega|,$$

where

$$\begin{aligned} \widetilde{\mathcal{G}}_\sigma(\varphi, \mathbf{n}) &= \int_\Omega \left(|\nabla\varphi - i\mathbf{n}\varphi|^2 + \frac{\widetilde{g}}{2}(1 - |\varphi|^2)^2 + \widetilde{K}|\nabla\mathbf{n}|^2 + \sigma n_2^2 \right) dxdy \qquad (27)\\ &=: \int_\Omega g(\varphi, \nabla\varphi, \mathbf{n})\,dxdy. \end{aligned}$$

To show (a), it suffices to prove that

$$\widetilde{\mathcal{G}}_\sigma(\varphi_\sigma, \mathbf{n}_\sigma) \le C\sqrt{\sigma} \tag{28}$$

for some positive constant C. We define a test map;

$$\varphi = e^{ix}, \qquad \mathbf{n} = (\sin\phi, \cos\phi)$$

where $\phi|_\Gamma = 0$ so that $\mathbf{n}|_\Gamma = \mathbf{e}_2$, here Γ is a top and bottom plates. We consider $\Omega_\eta = \{(x,y) \in \Omega : dist((x,y),\Gamma) < \eta\}$ for small parameter η yet to be determined. Define $\phi = \frac{\pi}{2}$ in $\Omega - \Omega_\eta$ and $|\nabla\phi| \le \frac{C}{\eta}$ for some constant C. Then we have

$$\int_{\Omega-\Omega_\eta} g(\varphi, \nabla\varphi, \mathbf{n})\, dxdy = 0.$$

In Ω_η, we have

$$\int_{\Omega_\eta} g(\varphi, \nabla\varphi, \mathbf{n})\, dxdy = \int_{\Omega_\eta} (2 - 2\sin\phi + \widetilde{K}|\nabla\phi|^2 + \sigma\cos^2\phi)\, dxdy$$

$$\le \big(4 + \widetilde{K}\frac{C^2}{\eta^2} + \sigma\big)|\Omega_\eta| \le C_0\left(\frac{C^2\widetilde{K} + (\sigma+4)\eta^2}{\eta}\right) \tag{29}$$

for some constant C_0. We choose

$$\eta = \frac{C\sqrt{\widetilde{K}}\sqrt{\sigma}}{\sigma+4}.$$

This, together with (29), gives

$$\begin{aligned}\widetilde{\mathcal{G}}_\sigma(\varphi,\mathbf{n}) &\le 2C\sqrt{\widetilde{K}}C_0\left(\sqrt{\sigma} + \frac{2}{\sqrt{\sigma}}\right)\\ &\le 3CC_0\sqrt{\widetilde{K}\sigma}\end{aligned}$$

for σ large. This gives the first part of the theorem. Now we claim that there is a subsequence of $\mathbf{n}_\infty$, not relabeled, such that $\mathbf{n}_\sigma \to \mathbf{n}_\infty$ in $L^1(\Omega)$ as $\sigma \to \infty$ and $|\mathbf{n}_\infty| = 1$. From (27) and (28), we have

$$\int_\Omega \left(\frac{\tilde{K}}{\sqrt{\sigma}}|\nabla\mathbf{n}_\sigma|^2 + \sqrt{\sigma}|(n_\sigma)_2|^2\right) \le C.$$

Writing $\mathbf{n}_\sigma = (u_\sigma, v_\sigma) \in \mathbb{S}^1$ and using $0 \le 1 - u_\sigma^2 \le 1$, we have

$$\frac{\tilde{K}}{\sqrt{\sigma}}\int_\Omega |\nabla u_\sigma|^2 + \frac{\sqrt{\sigma}}{2}\int_\Omega (1-u_\sigma^2)^2 \le C, \tag{30}$$

$$\frac{\sqrt{\sigma}}{2}\int_\Omega |v_\sigma|^2 < C. \tag{31}$$

Functional (30) is a classical Modica-Mortola model [17] for the study of phase transitions. Following [18], one can see that there exist a subsequence, still labelled u_σ, and $u_\infty \in BV(\Omega : \{\pm 1\})$ such that

$$u_\sigma \to u_\infty \quad \text{in } L^1(\Omega).$$

To prove this, define the function

$$\Phi(x) = \int_{-1}^{x} |1 - t^2|\, dt.$$

It follows from (30) that

$$\int_\Omega |D\Phi(u_\sigma)| = \int_\Omega |\nabla u_\sigma||1 - u_\sigma^2| \le C.$$

If we define $z_\sigma = \Phi(u_\sigma)$, it follows from this bound and $|u_\sigma| \le 1$ that $\{z_\sigma\}$ is bounded in the BV-norm. Thus there exists $z_\infty \in L^1(\Omega)$ and a subsequence (not relabeled) such that $z_\sigma \to z_\infty$ in $L^1(\Omega)$ and pointwise a.e. in Ω. Since the function

Φ is strictly increasing and continuous on $[-1,1]$, its inverse, denoted by Ψ, is continuous. Define $u_\infty = \Psi(z_\infty)$. Since $u_\sigma = \Psi(z_\sigma)$ and $|u_\sigma| \le 1$, it follows by the Dominated Convergence Theorem that $u_\sigma \to u_\infty$ in $L^p(\Omega)$ for all $1 \le p < \infty$. As a consequence of (30) and Fatou's lemma, we get that $|u_\infty| = 1$ a.e. in Ω, and since $z_\infty \in BV(\Omega)$, then $u_\infty \in BV(\Omega : \{\pm 1\})$.

This, together with the inequality (31) and $|u_\sigma|, |v_\sigma| \le 1$, concludes that $\{\mathbf{n}_\sigma\}$ is precompact in $L^p(\Omega)$ for all $p < \infty$ and thus part (b) is proved. □

Now we find an approximation for the smectic order parameter φ at high fields.

Theorem 4.2. *Let $(\varphi_\sigma, \mathbf{n}_\sigma)$ be a minimizer of $\mathcal{G}_\sigma(\varphi, \mathbf{n})$. Then there is a subsequence, still labeled $(\varphi_\sigma, \mathbf{n}_\sigma)$ and $(\varphi_\infty, \mathbf{n}_\infty) \in W^{1,2}(\Omega) \times \mathbf{L}^2(\Omega, \mathcal{S}^1)$ such that*

$$(\varphi_\sigma, \mathbf{n}_\sigma) \to (\varphi_\infty, \mathbf{n}_\infty) \quad \text{in} \quad L^2(\Omega) \times \mathbf{L}^2(\Omega)$$

as $\sigma \to \infty$. We also have $u_\infty = u_\infty(x)$ with $|u_\infty| = 1$ and $v_\infty = 0$ where $\mathbf{n}_\infty = (u_\infty, v_\infty)$ and φ_∞ can be written as

$$\varphi_\infty = ce^{i\phi}$$

for some $|c| = 1$ and $\phi = \int_0^x u_\infty(s)ds$.

Proof. We use a test function, $\varphi_0 = e^{ix}$ and a global minimizer $\mathbf{m}_\sigma$ of $\mathcal{F}_\sigma(\mathbf{n})$ such that $\mathbf{m}_\sigma \to \mathbf{e}_1$ in $L^2(\Omega)$ by (26). Then

$$\mathcal{G}_\sigma(\varphi_\sigma, \mathbf{n}_\sigma) \le \mathcal{G}_\sigma(\varphi_0, \mathbf{m}_\sigma) = \int_\Omega |\mathbf{e}_1 - \mathbf{m}_\sigma|^2 \, dxdy + \mathcal{F}_\sigma(\mathbf{m}_\sigma).$$

Thus,

$$\begin{aligned}\int_\Omega \left(|\nabla\varphi_\sigma - i\mathbf{n}_\sigma\varphi_\sigma|^2 + \frac{\widetilde{g}}{2}(1-|\varphi_\sigma|^2)^2 \right) dxdy \\ &\le \int_\Omega |\mathbf{e}_1 - \mathbf{m}_\sigma|^2 \, dxdy + \mathcal{F}_\sigma(\mathbf{m}_\sigma) - \mathcal{F}_\sigma(\mathbf{n}_\sigma) \\ &\le \int_\Omega |\mathbf{e}_1 - \mathbf{m}_\sigma|^2 \, dxdy\end{aligned}$$

since $\mathbf{m}_\sigma$ is a minimizer of $\mathcal{F}_\sigma$. Also, from (26), we have

$$\int_\Omega \left(|\nabla\varphi_\sigma - i\mathbf{n}_\sigma\varphi_\sigma|^2 + \frac{\widetilde{g}}{2}(1-|\varphi_\sigma|^2)^2 \right) dxdy \to 0 \tag{32}$$

as $\sigma \to \infty$. From the second term, we have

$$\int_\Omega |\varphi_\sigma|^2 dxdy \le C.$$

Now from the first term, we have

$$\int_\Omega |\nabla\varphi_\sigma|^2 dxdy \le \int_\Omega |\mathbf{n}_\sigma|^2 |\varphi_\sigma|^2 dxdy \le C.$$

Then there is $\varphi_\infty \in W^{1,2}(\Omega)$ and a subsequence, not relabeled, such that $\varphi_\sigma \rightharpoonup \varphi_\infty$ in $W^{1,2}(\Omega)$ and $\varphi_\sigma \to \varphi_\infty$ in $L^2(\Omega)$. Then, from (32) and Theorem 4.1,

$$\begin{aligned}0 = \liminf_{\sigma\to\infty} \int_\Omega \left(|\nabla\varphi_\sigma - i\mathbf{n}_\sigma\varphi_\sigma|^2 + \frac{\widetilde{g}}{2}(1-|\varphi_\sigma|^2)^2 \right) dxdy \\ &\ge \int_\Omega \left(|\nabla\varphi_\infty - i\mathbf{n}_\infty\varphi_\infty|^2 + \frac{\widetilde{g}}{2}(1-|\varphi_\infty|^2)^2 \right) dxdy.\end{aligned}$$

One can see that,

$$|\varphi_\infty| = 1 \qquad \text{and} \qquad \nabla\varphi_\infty = i\mathbf{n}_\infty\varphi_\infty. \tag{33}$$

We claim that

$$\varphi_\infty = ce^{i\phi}$$

where $\phi(x) = \int_0^x u_\infty(s)ds$ for some constant c such that $|c| = 1$, applying the method of proof in [16]. At a point x_0 in Ω, we may represent φ_∞ by $\rho e^{i\phi}$ with $\rho > 0$ on $N(x_0)$, a neighborhood of x_0. Then (33) implies

$$\rho = 1 \qquad \text{and} \qquad \nabla\phi = \mathbf{n}_\infty = \begin{pmatrix} u_\infty \\ v_\infty \end{pmatrix} \tag{34}$$

on $N(x_0)$. It follows from Theorem 4.1 that $|u_\infty| = 1$ and $v_\infty = 0$ and hence we have $\phi = \phi(x)$ and $u_\infty = u_\infty(x)$. Thus we get on $N(x_0)$

$$\varphi_\infty = ce^{i\phi}$$

where $\phi(x) = \int_0^x u_\infty(s)ds$ for some constant c such that $|c| = 1$. Since c does not depend on x_0 in a rectangular domain Ω, the claim is proved. □

5. **Conclusion.** In this work, we have investigated the magnetic field effects on the smectic A liquid crystals by studying the complex de Gennes free energy. We perform numerical simulations for the gradient flow of the free energy with strong anchoring condition on the director and two boundary conditions on the smectic order parameter: Dirichlet and natural boundary conditions. Employing the natural boundary condition lowers the critical field for the undulations by allowing the fluctuation of the smectic order density near the bounding cells. The director field and layer structures with smectic order density are illustrated in various magnetic field strengths by numerical simulations. We further analyze minimizers of the free energy at the high field regime, which agrees the description of director and smectic order parameter from numerical simulations.

Acknowledgments. The authors would like to thank the anonymous reviewers for their valuable comments and suggestions to improve the quality of the paper. The work of Carlos J. García-Cervera is supported by NSF grants DMS-0645766 and DMS-0908538. The work of Sookyung Joo is supported by NSF grant DMS-1120637. S. Joo acknowledges the hospitality of the Issac Newton Institute where part of the work has been done. She also would like to express her gratitude to T. Sluckin for many fruitful discussions at the Issac Newton Institute.

REFERENCES

[1] V. G. Čigrinov, *Electrooptic Effects in Liquid Crystal Materials*, Springer, 1996.
[2] P. G. de Gennes, An analogy between superconductors and smectics A, *Solid State Communications*, **10** (1972), 753–756.
[3] P. G. de Gennes, *The Physics of Liquid Crystals*, International Series of Monographs on Physics, Clarendon Press, 1974.
[4] W. E and X. P. Wang, Numerical methods for the Landau–Lifshitz equation, *SIAM J. Numer. Anal.*, **38** (2000), 1647–1665.
[5] M. Frigo and S. G. Johnson, The design and implementation of FFTW3, *Proceedings of the IEEE*, **93** (2005), 216–231.
[6] C. J. García-Cervera and S. Joo, Analytic description of layer undulations in smectic *A* liquid crystals, *Arch. Ration. Mech. Anal.*, **203** (2012), 1–43.
[7] C. J. García-Cervera and S. Joo, Analysis and simulations of the Chen-Lubensky energy for smectic liquid crystals: Onset of undulations, *Commun. Math. Sci.*, **12** (2014), 1155–1183.

[8] T. Giorgi, C. J. García-Cervera and S. Joo, Sawtooth profile in smectic *A* liquid crystals, *submitted*.
[9] E. Giusti, *Minimal Surfaces and Functions of Bounded Variation*, Monographs in Mathematics, 80, Birkhäuser Verlag, Basel, 1984.
[10] W. Helfrich, Electrohydrodynamic and dielectric instabilities of cholesteric liquid crystals, *The Journal of Chemical Physics*, **55** (1971), 839–842.
[11] J. P. Hurault, Static distortions of a cholesteric planar structure induced by magnetic or ac electric fields, *The Journal of Chemical Physics*, **59** (1973), 2068–2075.
[12] T. Ishikawa and O. D. Lavrentovich, Undulations in a confined lamellar system with surface anchoring, *Phys. Rev. E*, **63** (2001), 030501.
[13] T. Ishikawa and O. D. Lavrentovich, Defects and undulation in layered liquid crystals, in *Defects in Liquid Crystals: Computer Simulations, Theory and Experiments* (eds. O. D. Lavrentovich, P. Pasini, C. Zannoni and S. Žumer), NATO Science Series, 43, Springer Netherlands, 2001, 271–300.
[14] T. Ishikawa and O. Lavrentovich, Dislocation profile in cholesteric finger texture, *Physical Review E*, **60** (1999), R5037.
[15] O. Lavrentovich, M. Kleman and V. M. Pergamenshchik, Nucleation of focal conic domains in smectic a liquid crystals, *Journal de Physique II*, **4** (1994), 377–404.
[16] F. Lin and X. B. Pan, Magnetic field-induced instabilities in liquid crystals, *SIAM J. Math. Anal.*, **38** (2006/07), 1588–1612.
[17] L. Modica and S. Mortola, Un esempio di Γ-convergenza, *Boll. Un. Mat. Ital.*, **14** (1977), 285–299.
[18] L. Modica, The gradient theory of phase transitions and the minimal interface criterion, *Arch. Rational Mech. Anal.*, **98** (1987), 123–142.
[19] B. I. Senyuk, I. I. Smalyukh and O. D. Lavrentovich, Undulations of lamellar liquid crystals in cells with finite surface anchoring near and well above the threshold, *Phys. Rev. E*, **74** (2006), 011712.
[20] M. Struwe, Heat-flow methods for harmonic maps of surfaces and applications to free boundary problems, in *Partial Differential Equations* (Rio de Janeiro, 1986), Lecture Notes in Math., 1324, Springer, Berlin, 1988, 293–319.

Received December 2013; revised March 2015.

E-mail address: cgarcia@math.ucsb.edu
E-mail address: sjoo@odu.edu